Journal of Alloys and Compounds 480 (2009) 220–224

Contents lists available at ScienceDirect

Journal of Alloys and Compounds

journal homepage: www.elsevier.com/locate/jallcom

Effects of Y_2O_3 addition on the phase evolution and thermophysical properties of lanthanum zirconate

Zhenhua Xu[a,b,c], Limin He[c], Xinghua Zhong[a,b], Jiangfeng Zhang[a,b], Xiaolong Chen[a,b], Hongmei Ma[a], Xueqiang Cao[a,*]

[a] State Key Laboratory of Rare Earth Resource Utilization, Changchun Institute of Applied Chemistry, Chinese Academy of Sciences, Changchun 130022, China
[b] Graduate School of Chinese Academy of Sciences, Beijing 100039, China
[c] Beijing Institute of Aeronautical Materials, Department 5, P.O. Box 81-5, Beijing 100095, China

ARTICLE INFO

Article history:
Received 22 January 2009
Received in revised form 16 February 2009
Accepted 17 February 2009
Available online 26 February 2009

Keywords:
Lanthanum zirconate
Yttria
Thermal expansion
Sintering-resistance
Ceramics

ABSTRACT

Lanthanum zirconate ($La_2Zr_2O_7$, LZ) powders with the addition of various Y_2O_3 contents for potential thermal barrier coatings (TBCs) application were synthesized by solid-state reaction. The structure evolution, sintering-resistance and thermophysical properties of the synthesized powders and sintered ceramics were systematically studied. X-ray diffraction (XRD) results indicate that LZ containing 3–12 wt.% Y_2O_3 mainly keeps a pyrochlore-type structure, and two new phases of $LaYO_3$ and $Y_{0.18}Zr_{0.82}O_{1.91}$ are also detected. Raman spectra confirm that the higher the Y_2O_3 content, the easier is the formation of $LaYO_3$. With the increase of Y_2O_3 content, the linear thermal expansion coefficients (TEC) of different La_2O_3–ZrO_2–Y_2O_3 ceramics may gradually decrease. Additionally, LZ ceramics doped with 3 wt.% Y_2O_3 have the lowest relative density and the highest sintering-resistance among all samples, implying that it is the best candidate for TBCs among those samples in this investigation.

1. Introduction

In recent years, further increase in thrust-to-weight ratio and higher gas temperature are required in advanced turbine engines. In order to meet this requirement, ceramic thermal barrier coatings (TBCs) are widely used for thermal insulation against hot combustion gases. The application of TBCs greatly enhances the operation temperature and thermal efficiency of gas turbines, and reduces fuel consumption and gas emission at elevated temperatures [1–4]. State-of-the-art TBCs are based on yttria-stabilized zirconia (YSZ), which is applied on engine components by atmospheric plasma spraying (APS) or electron beam-physical vapor deposition (EB–PVD) [5].

YSZ, especially zirconia containing 8 wt.% yttria (8YSZ) is currently used as the standard material of TBCs due to its low thermal conductivity (2.1 $W m^{-1} K^{-1}$), relatively high thermal expansion coefficient ($11 \times 10^{-6} K^{-1}$) and chemical inertness in combustion atmospheres [6]. However, the major disadvantage of 8YSZ is the limited operation temperature of 1473 K for the long-term application [7]. At higher temperatures, the t'-tetragonal phase transforms into the tetragonal and the cubic ($t+c$) phases. The t'-tetragonal phase means non-equilibrium tetragonal phase, which is still stable below 1473 K after long-term exposure. During cooling, the t-phase will further transform into the monoclinic (m) phase, giving rise to the volume increase and resulting in the formation of cracks in the coating [8]. In order to overcome these disadvantages of 8YSZ and meet the ambitious designing, it is urgently needed to develop new candidate materials with even lower thermal conductivity, higher operation temperature, better sintering-resistance and phase stability at even higher temperature for future improvements in engine's performance.

Among the interesting candidates for TBCs, rare earth zirconates have been investigated, and they have been proved to be significant for the top coating materials. Among these materials with pyrochlore structures and high melting points, lanthanum zirconate ($La_2Zr_2O_7$, LZ) shows promising thermo-physical properties and has attracted a great attention. LZ has a lower thermal conductivity (1.56 $W m^{-1} K^{-1}$) than 8YSZ, a cubic pyrochlore structure which is stable up to its melting point (2573 K), and it has been proposed as a promising TBCs material [6,8–10]. LZ coating has been fabricated by EB–PVD [6,10–12], La and Zr are not equally distributed in the coating during deposition due to evaporation differences of La_2O_3 and ZrO_2. Presence of a lower vapor pressure oxide such as Y_2O_3 helps to moderate the excessive vapor pressure condition during deposition as well as the growth conditions in favor of pertinent pyrochlore structure formation [6,13]. B. Saruhan et al. [6,13] confirmed that Y_2O_3 addition in LZ could improve the chemical homogeneity of its coating.

* Corresponding author. Tel.: +86 431 85262285; fax: +86 431 85262285.
E-mail address: xcao@ciac.jl.cn (X. Cao).

0925-8388/$ – see front matter © 2009 Elsevier B.V. All rights reserved.
doi:10.1016/j.jallcom.2009.02.048

Table 1
Chemical composition and thermal expansion coefficients (α, 298–1673 K) of La_2O_3–ZrO_2–Y_2O_3 ceramics.

Sample codes	Chemical composition (wt.%)				Theoretical density (g cm^{-3})	α ($\times10^{-6}$ K^{-1})
	La_2O_3	ZrO_2	Y_2O_3	Formula		
A0	56.93	43.07	0	$La_2Zr_2O_7$	6.05	9.27
A1	55.22	41.78	3	$La_2(Zr_{0.9216}Y_{0.0784})_2O_7$	6.00	–
A2	53.51	40.49	6	$La_2(Zr_{0.8382}Y_{0.1618})_2O_7$	5.96	9.15
A3	51.81	39.19	9	$(La_{0.9177}Y_{0.0883})_2(Zr_{0.8382}Y_{0.1618})_2O_7$	5.89	–
A4	50.10	37.90	12	$(La_{0.8167}Y_{0.1833})_2(Zr_{0.8382}Y_{0.1618})_2O_7$	5.78	9.01

However, no data on the phase evolution and thermophysical properties of LZ doped with various Y_2O_3 contents are reported in open literatures up to date, and the optimized content of Y_2O_3 is not available. In the present work, LZ powders doped by various Y_2O_3 contents for potential TBCs application are synthesized by solid-state reaction, the structure evolution, sintering-resistance and thermophysical properties of LZ bulk ceramics doped by various Y_2O_3 contents are investigated in detail.

2. Experimental

In the present study, rare earth oxides powders (La_2O_3, ZrO_2 and Y_2O_3) were heat-treated at 1273 K for 2 h in air before weighting as rare earth oxides are hygroscopic. Different La_2O_3–ZrO_2–Y_2O_3 ceramics with the desired composition were synthesized by solid-state reaction at 1673 K for 12 h with La_2O_3 (99.99%, Chenghai Chemicals of Guangdong), ZrO_2 (99.9%, Chenghai Chemicals of Guangdong) and Y_2O_3 (99.9%, Chenghai Chemicals of Guangdong) as the starting materials. Compositions of various La_2O_3–ZrO_2–Y_2O_3 ceramics (designated with the sample codes of A0-A4, respectively) used in this investigation were listed in Table 1.

The crystal structures of the sintered bulk ceramics were characterized by X-ray diffraction (XRD, Bruker D8 Advance) with nickel-filtered Cu Kα radiation at a scan rate of 10°/min, and the diffraction patterns in 2θ range of 26.5–34.5° were recorded in a step scan mode with a step width of 0.02° and a step time of 2 s. The theoretical density of sintered specimens was calculated using lattice parameters acquired from XRD results. The bulk densities of the specimens were determined by mass and dimensions measurements. Small bars of sintered specimens were prepared by cold pressing followed by sintering at different temperatures for 6 h; the volume shrinkages were then measured.

The linear thermal expansion coefficients of the representative sintered ceramics with a dimension of 25 mm × 5 mm × 2 mm were determined with a high-temperature dilatometer (Netzsch 402C, Germany) from room temperature to 1673 K in air atmosphere. Data were continuously recorded at a heating rate of 5 K/min during heating, and they were corrected using the known thermal expansion coefficient of a certified standard alumina. Raman spectrum was recorded at room temperature with T64000 modular triple Raman system (Horiba Jobin Yvon, France). The 514.5 nm line of an argon ion laser (Stabilite 2017, Spectra-Physics Lasers Inc., USA) was used as the excitation line. Laser power of 5 mW was incident on the sample in a 2 μm diameter spot through a standard microscope objective lens. The Raman spectrum was collected with a data point acquisition time of 90 s and a spectral range of 100–1000 cm^{-1}.

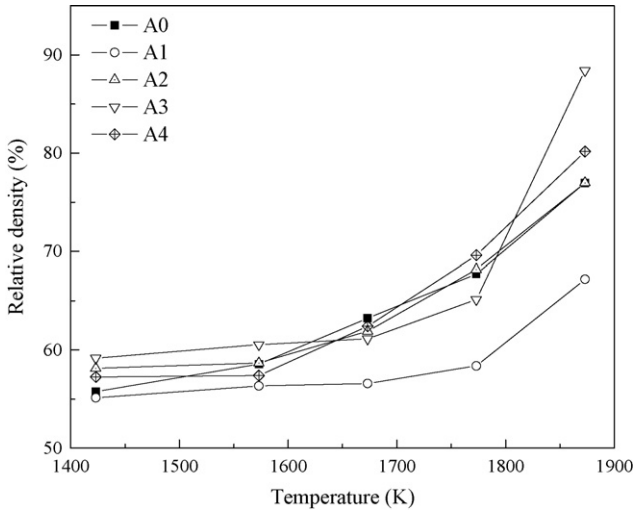

Fig. 1. Variation in relative densities with sintering temperature.

3. Results and discussion

3.1. Characterization of La_2O_3–ZrO_2–Y_2O_3 bulk ceramics

Fig. 1 shows the variations in relative densities of La_2O_3–ZrO_2 (sample A0) and various La_2O_3–ZrO_2–Y_2O_3 (samples A1–A4) bulk ceramics with sintering temperature. Clearly, all specimens sintered at 1423 K for 6 h have lower relative densities than those sintered at 1873 K for 6 h. The relative densities of all specimens sintered at each temperature do not increase with the increase of Y_2O_3 content in raw materials. Sample A3 sintered at 1873 K for 6 h has the highest relative density of ~90%, and Sample A1 has the lowest density. It is probably attributed to swell of specimen on heating and low diffusion mobility of ions in its sublattice at 1873 K [14]. It indicates that the incorporation of 3 wt.% Y_2O_3 to the La_2O_3–ZrO_2 system can lower the sintering densification behavior.

The XRD patterns of the LZ ceramics doped with and without Y_2O_3 after being sintered at 1673 K for 12 h are shown in Fig. 2. Samples A0–A4 exhibit only a pyrochlore-type lattice, which is characterized by the presence of typical super-lattice peaks at 2θ values of about 14° (1 1 1), 28° (3 1 1), 37° (3 3 1) and 45° (511) using Cu Kα radiation [15,16]. It can be carefully seen from Fig. 2 that the diffraction patterns in the 2θ range of 26.5–34.5° seem to be different. Therefore, in the interest 2θ ranges of 26.5–34.5°, fine stepwise XRD patterns of La_2O_3–ZrO_2 (sample A0) and various La_2O_3–ZrO_2–Y_2O_3 (samples A1–A4) bulk ceramics from Fig. 2 are shown in Fig. 3. Peak I of A0 disappears and the intensity of Peak

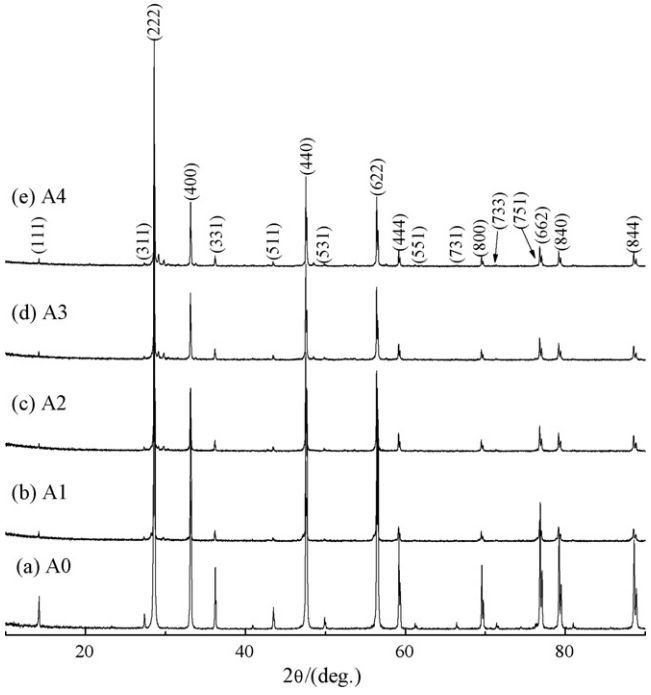

Fig. 2. XRD patterns of samples A0–A4 bulk ceramics sintered at 1673 K for 12 h.

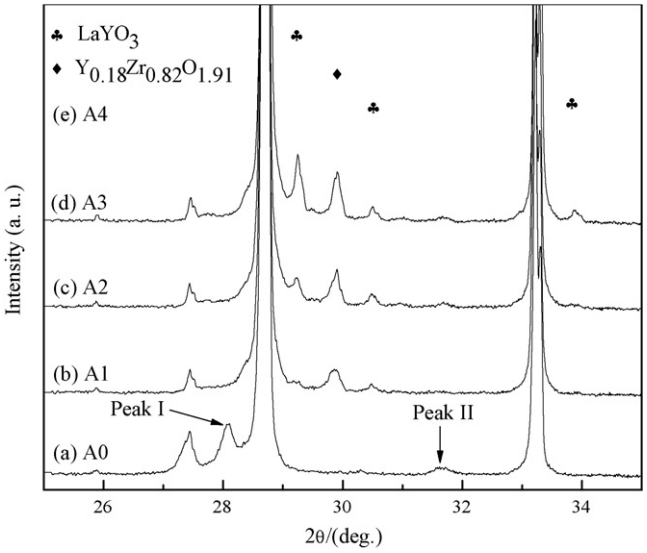

Fig. 3. Fine stepwise XRD patterns (26.5–34.5°) of samples A0–A4 bulk ceramics sintered at 1673 K for 12 h.

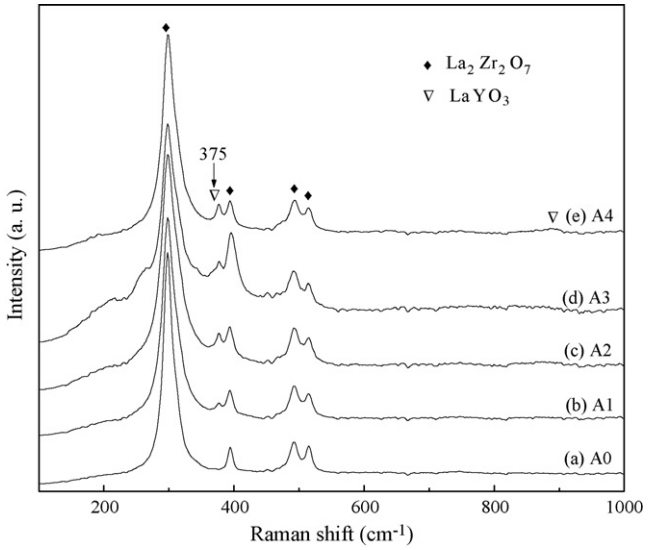

Fig. 4. Raman spectra of samples A0–A4 bulk ceramics after being sintered at 1673 K for 12 h.

II is also weakened after the doping of Y_2O_3 for A1–A4. In samples A1–A4, two new phases of $LaYO_3$ and $Y_{0.18}Zr_{0.82}O_{1.91}$ are formed, and the intensity of peaks located at 29.24°, 29.91° and 30.50° are gradually enhanced. Additionally, one weak peak of $LaYO_3$ located at 33.86° is observed in A3 and A4. The following may be the reasons for these results:

(1) The chemical reactions:

$$La_2Zr_2O_7 + Y_2O_3 = 2LaYO_3 + 2ZrO_2 \quad (1)$$

$$0.18Y_2O_3 + 1.64ZrO_2 = 2Y_{0.18}Zr_{0.82}O_{1.91} \quad (2)$$

The higher the Y_2O_3 content, the easier are the chemical reactions in Eqs. (1) and (2).

(2) La^{3+} in LZ is partially substituted by Y^{3+}; it will cause the additional chemical reaction which can be expressed as:

$$La_2O_3 + Y_2O_3 = 2LaYO_3 \quad (3)$$

Laser Raman spectroscopy is a powerful tool to investigate chemical composition in ceramic materials [17]. Fig. 4 shows the Raman spectra of LZ ceramics doped with and without Y_2O_3 after being sintered at 1673 K for 12 h in the Raman shift range of 100–1000 cm^{-1} at room temperature. For samples A0–A4, four Raman bands at 299, 395, 490 and 515 cm^{-1} are visible. These Raman bands are the characteristics of LZ-type structure, which is consistent with the previous results [18]. One Raman band at 375 cm^{-1} is also detected in A1–A4, which is the characteristics of $LaYO_3$ according to the Raman spectrum of pure $LaYO_3$. Meanwhile, the peak intensity of $LaYO_3$ is gradually increased with the increase of Y_2O_3 content, implying that the addition of Y_2O_3 is quite beneficial to the formation of $LaYO_3$. This result is in good agreement with the XRD results shown in Fig. 3. On the other hand, Yamaguchi et al. [19] reported that $LaYO_3$ was still stable when the sintering temperature was below 1723 K, implying that it is probably suitable for TBCs application. Therefore, compared to the LZ ceramics, the phase stabilities of LZ ceramics after doping with various Y_2O_3 contents basically keep unchanged even the sintered temperature is only at 1673 K.

The lattice parameters calculated from XRD patterns of samples A0–A4 (Fig. 2) in relation to the pyrochlore unit cell are shown in Fig. 5. The approximately linear increase of lattice parameters with the increase of Y_2O_3 content for A0–A2 is observed because Y^{3+} (0.089 nm) has a larger ionic radius than Zr^{4+} (0.072 nm). However, according to the fitted curves determined from the distribution of the experimental points in Fig. 5, the highest Y_2O_3 content in La_2O_3–ZrO_2–Y_2O_3 ceramics is about 6.02 wt.%. With the increase of Y_2O_3 content from 6.02 wt.% to 12 wt.%, lattice parameters are reduced. La^{3+} (1.06 Å) has a larger ionic radius than Y^{3+}, the decrease of lattice parameters with the increase of Y_2O_3 content may be a result of the substitution of La^{3+} by Y^{3+}. By taking into account the lattice parameter, the actual chemical formulas and theoretical densities of samples A0–A4 are calculated and listed in Table 1. In $Ln_2Zr_2O_7$, the crystal structure is firstly determined by the ionic radius ratio of $r(Ln^{3+})/r(Zr^{4+})$. The pyrochlore structure stability at an atmospheric pressure in zirconates is limited to the range of $1.46 \le r(Ln^{3+})/r(Zr^{4+}) \le 1.78$ [20]. The ionic radius of Zr^{4+} is 0.072 nm when the coordination number is 6; however, the ionic radius of La^{3+} and Y^{3+} are 0.106 and 0.089 nm in an eight-fold coordination, respectively. The calculated values of $r(Ln^{3+})/r(Zr^{4+})$ are 1.47, 1.60, 1.75, 1.74 and 1.69 for samples A0–A4, respectively. Therefore, it

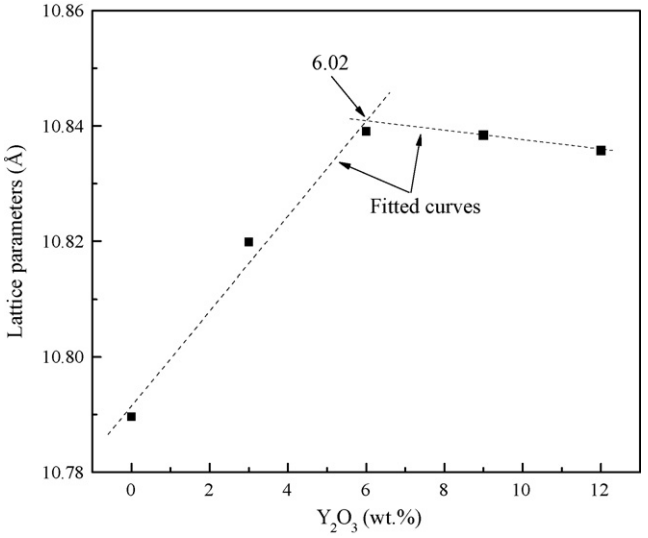

Fig. 5. Lattice parameters derived from XRD peaks of samples A0–A4 (Fig. 2) with different Y_2O_3 contents.

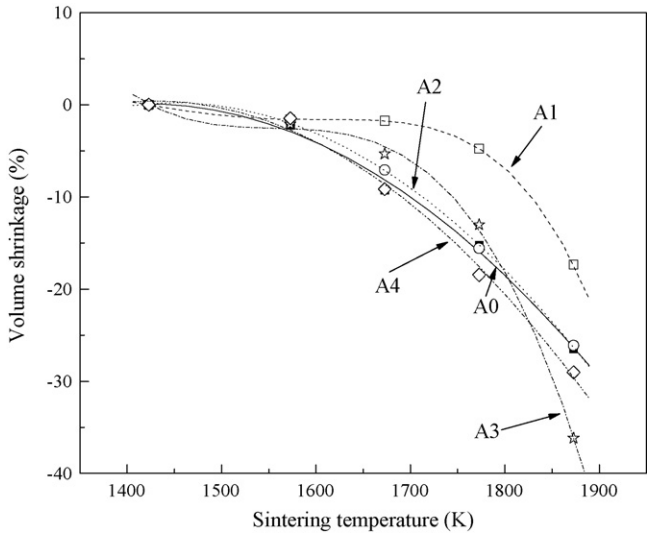

Fig. 6. Volume shrinkages of samples A0–A4 after being sintered at different temperature for 6 h.

further proves that samples A0–A4 mainly keep a pyrochlore-type structure.

3.2. Thermophysical properties of La_2O_3–ZrO_2–Y_2O_3

The volume shrinkages of A0–A4 at elevated temperatures are compared in Fig. 6. The volume shrinkage with the increase of sintering temperature seems to basically obey the parabolic law, which is similar to the result of LZ doped with CeO_2 as reported in Ref. [21]. The volume shrinkages of A0 and A2 are identical. The largest shrinkage after being sintered at 1873 K for 6 h is observed in A3. A1 has the highest sintering-resistance among all these samples.

The thermal expansion coefficient (TEC) is an important thermophysical property for La_2O_3–ZrO_2–Y_2O_3 ceramics. The results of the dilatometric measurement for different La_2O_3–ZrO_2–Y_2O_3 bulk ceramics with calibration are shown in Fig. 7. The typical linear expansion is observed for three different La_2O_3–ZrO_2–Y_2O_3 ceramics between 298 and 1673 K, and apparently there is no phase transformation in this temperature range.

The average linear TEC (α) is defined as the value of the relative length change in the temperature range of $T_1 < T < T_2$, as described by the following equation [22]:

$$\alpha = \frac{(L_2 - L_1)}{L_0(T_2 - T_1)} = \frac{\Delta L}{L_0 \Delta T} \quad (1)$$

where L_0, L_1 and L_2 are the lengths of the specimen at temperatures of T_0 (25 K), T_1 and T_2, respectively. The average linear TECs of A0, A2 and A4 bulk materials are shown in Table 1 in the temperature range of 298–1473 K. TECs of A0–A4 are between 9.01×10^{-6} 9.27×10^{-6} K^{-1}, and basically decrease with the increase of Y_2O_3 content, and A1 has the highest value among those samples A1–A4. In the pyrochlore-type rare earth zirconates, oxygen vacancies are distributed in long-range ordering arrangements, therefore facilitate to some extent the thermal expansion related to the strength of the ionic bonds between rare earth cations and oxygen anions. It is important to note that there are some structural features (e.g., defects such as oxygen vacancy $V_{\ddot{o}}$, substitution cation Y^{3+} and other imperfections in the lattice such as pores or varying properties in thermal expansion along with different orientations) that have a significant effect on the overall TECs of different La_2O_3–ZrO_2–Y_2O_3 ceramics [23,24].

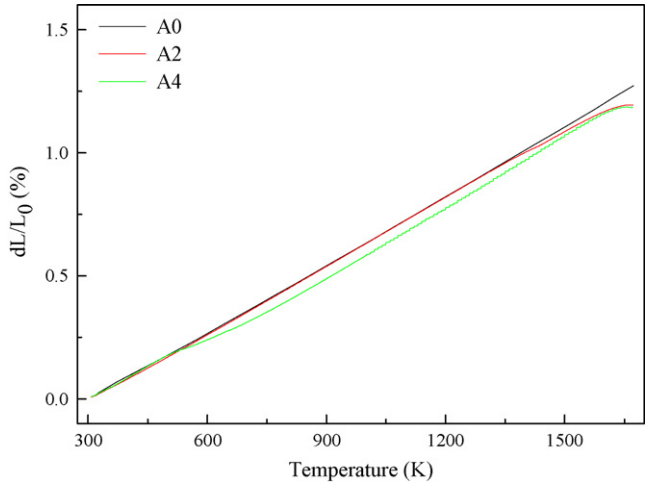

Fig. 7. Calibrated dilatometric data for samples A0, A2 and A4 bulk ceramics as a function of temperature.

4. Conclusions

The composite oxides of La_2O_3–ZrO_2–Y_2O_3 bulk ceramics as novel TBCs material were synthesized by solid-state reaction, and the phase structural evolution, sintering-resistance and thermophysical properties of LZ bulk ceramics doped by various Y_2O_3 contents were systematically investigated. From our experimental investigation, the following conclusions can be obtained:

(1) The incorporation of 3–12 wt.% Y_2O_3 to LZ ceramics mainly keeps a pyrochlore-type structure. Two new phases of $LaYO_3$ and $Y_{0.18}Zr_{0.82}O_{1.91}$ are also detected in the La_2O_3–ZrO_2–Y_2O_3 ceramics, and the higher the Y_2O_3 content, the easier is the formation of them.
(2) LZ ceramics doped with 3 wt.% Y_2O_3 has the lowest relative density and the highest sintering-resistance ability among all the samples.
(3) The average linear thermal expansion coefficients of different La_2O_3–ZrO_2–Y_2O_3 ceramics may gradually decrease with the increase of Y_2O_3 content, and their values are basically located within the range of $9.01–9.27 \times 10^{-6}$ K^{-1} from room temperature to 1673 K.

Acknowledgement

This work was financially supported by the projects of NSFC-50825204.

References

[1] N.P. Padture, M. Gell, E.H. Jordan, Science 296 (2002) 280–284.
[2] M. Belmonte, Adv. Eng. Mater. 8 (2006) 693–703.
[3] Z.-G. Liu, J.H. Ouyang, Y. Zhou, J. Alloys Compd. (2008), doi:10.1016/j.jallcom.2008.04.042.
[4] Z.-G. Liu, J.H. Ouyang, B.H. Wang, Y. Zhou, J. Li, J. Alloys Compd. 466 (2008) 39–44.
[5] W.A. Nelson, R.M. Orenstein, J. Therm. Spray Technol. 6 (1) (1997) 176–180.
[6] B. Saruhan, P. Francois, K. Fritscher, U. Schulz, Surf. Coat. Technol. 182 (2004) 175–183.
[7] W. Ma, S.K. Gong, H.B. Xu, X.Q. Cao, Surf. Coat. Technol. 200 (2006) 5113–5118.
[8] X.Q. Cao, R. Vassen, W. Jungen, S. Schwartz, F. Tietz, D. Stöve, J. Am. Ceram. Soc. 84 (9) (2001) 2086–2090.
[9] R. Vassen, X.Q. Cao, F. Tietz, D. Basu, D. Stöve, J. Am. Ceram. Soc. 83 (8) (2000) 2023–2028.
[10] K. Bobzin, E. Lugscheider, N. Bagcivan, High Temp. Mater. Proc. 10 (2006) 103–108.
[11] Z.H. Xu, X.H. Zhong, J.F. Zhang, Y.F. Zhang, X.Q. Cao, L.M. He, Surf. Coat. Technol. 202 (2008) 4714–4720.
[12] K. Bobzin, E. Lugscheider, N. Bagcivan, Adv. Eng. Mater. 8 (2006) 653–657.

[13] B. Saruhan, K. Frischer, U. Schulz, Ceram. Eng. Sci. Proc. 24 (2003) 491–496.
[14] E.R. Andrievskaya, V.P. Redko, Mater. Sci. Eng. 518 (2006) 343–348.
[15] B.P. Mandal, A.K. Tyagi, J. Alloys Compd. 437 (2007) 260–263.
[16] Z.-G. Liu, J.H. Ouyang, Y. Zhou, J. Li, J. Alloys Compd. (2008), doi:10.1016/j.jallcom.2008.01.026.
[17] B.P. mandal, V. Grover, M. Roy, A.K. Tyagi, J. Am. Ceram. Soc. 90 (2007) 2961–2965.
[18] J. Nair, P. Nair, B.M. Docsburg, G.V. Ommen, R.H. Ross, A.J. Burggraaf, F. Mizukami, J. Am. Ceram. Soc. 82 (8) (1999) 2066–2072.
[19] O. Yamaguchi, H. Kawabata, H. Hashimoto, K. Shimizu, J. Am. Ceram. Soc. 70 (6) (1987) 131–132.
[20] M.A. Subramanian, G. Aravamudan, G.V. Subba Rao, Prog. Solid State Chem. 15 (1983) 55–143.
[21] X.Q. Cao, J.Y. Li, X.H. Zhong, J.F. Zhang, Y.F. Zhang, R. Vassen, D. Stoever, Mater. Lett. 62 (2008) 2667–2669.
[22] Z.-G. Liu, J.H. Ouyang, Y. Zhou, J. Mater. Sci. 43 (2008) 3596–3603.
[23] Z.-G. Liu, J.H. Ouyang, Y. Zhou, J. Alloys Compd. (2008), doi:10.1016/j.jallcom.2008.05.053.
[24] Z.-G. Liu, J.H. Ouyang, Y. Zhou, J. Li, X.L. Xia, Adv. Eng. Mater. 8 (2008) 754–758.